PAPER • **OPEN ACCESS**

Water recycling system based on adsorption by activated carbon synthesised from c. verum for space exploration; an estimated design

To cite this article: M N Ettish *et al* 2021 *IOP Conf. Ser.: Mater. Sci. Eng.* **1172** 012024

Water recycling system based on adsorption by activated carbon synthesised from c. verum for space exploration; an estimated design

M N Ettish[1], O Abuzalat[1], G S El-Sayyad[2] and M A Elsayed[1]

[1] Chemical Engineering Department, Military Technical College, Kobry Elkobbah, Cairo, Egypt.
[2] Drug Microbiology Laboratory, Drug Radiation Research Department, National Center for Radiation Research and Technology (NCRRT), Egyptian Atomic Energy Authority, Cairo,Egypt.

E-mail: mnasr4810@gmail.com

Abstract. Water recycling is a crucial component of space flights. In this study, c.verum, a low-cost agricultural by-product abundant in Egypt, which was not utilized before for the preparation of porous carbons, and its ability for recycling water in space stations was estimated. The prepared samples show high porosity and surface area by physical activation. The influences of the pyrolysis temperature and activation hold-up time on the activated carbon's porosity were studied. The BET surface area and the total pore volume of the prepared carbon were used as the criteria for selecting the optimum preparation parameters. The optimum temperature for pyrolysis was found to be at a temperature of 900°C, hold-up time of two-hour, a nitrogen flow rate of 150 cm3/min, and a heating rate of 10^0C/min. However, the optimum activation conditions were at a temperature of 900^0C, a CO2 flow rate of 150 cm3/min, a heating rate of 20^0C/min, and a hold-up time of 120 min. Equilibrium data is used for fitting to Freundlich, Langmuir, and Temkin isotherms models. The result revealed that the Langmuir model was the finest match for the equilibrium data, with an extreme monolayer adsorption capability of 12.37 mg/g at 25^0C. The maximum monolayer adsorption capacity decreased with increasing temperature confirmed the exothermic character of the adsorption interaction.

1. Introduction

Water is as crucial for existence in outer space as on Earth. Around 75% of the cost of established human life on the international space-station (ISS) is related to safe drinking water availability. A space traveler on the ISS uses approximately one gallon of water per day, and approximately estimated cost of $83,000 per gallon to lift to space, the costs will hastily be subjected to be increased in the future. Due to the high water recycling cost in space, NASA has developed and implemented research to design systems to recycle water at a low cost. Water recycling preserves costs down on resupply and makes space missions more Earth-independent and self-sufficient. However, more extended activities will demand much from the waste management system than from storage [1].

Activated carbon (AC) is broadly used for water effluent treatment. The activated carbon's utilization becomes restricted by its elevated cost due to using non-renewable and moderately-expensive origin. So, this has pointed to a growing concern in the construction of low-cost activated carbon. Additionally, the production method is a moderately-easy because of the great-reactivity of the performed biomass,

reducing the waste-disposal values and the harmful environmental influences. The manufacture of activated carbons from agricultural waste has gained much attention lately, such as almond shell, waste apricot, bean pod, cherry stone, date palm seed, rice husk, corn cob, coconut, and Olive stone.

The beginning substance's nature is an essential function in determining the formed activated carbon's quality, features, and characteristics [2].

Activated carbon synthesis from cinnamon sticks by-product has not been estimated before in the literature. As a result, looking at the viability of using a new by-product is the purpose of this study. Cinnamon sticks, as a candidate precursor to be used in the manufacturing of activated carbon by physical method. A study of its capability of removing Chlorpyrifos (CPS) - an organo-phosphorus organic compound.

2. Experimental section

2.1. Materials

Cinnamon sticks were purchased locally, as it is abundant in Egypt. N_2 and CO_2 gases were obtained from El Nasr Company. Sigma Aldrich delivered the acetonitrile. KZ Company supplied the chlorpyrifos.

2.2. Characterization and production of cinnamon sticks-based activated carbon (CSAC)

2.2.1. Pyrolysis process. The obtained raw-materials (Cinnamon sticks) were washed with purified water to discharge the contaminants after dissolving the unwanted substances, dehydrated at 110°C for 24 h, sieved after grounding to achieve particle size below 2 mm diameter. The dehydrated cinnamon granules were pyrolysed (tube furnace) at various temperatures (600-1000^0 C), with a heating flow of 10^{0}C/min for 120 min in the closeness of a nitrogen flow (150 $cm^3.min^{-1}$).

2.2.2. Activation progression. The char was activated at 900 ^{0}C with different holding time intervals, 30-150 min, using a CO_2 flow rate was 150 $cm^3.min^{-1}$, and heat rate was 20 $^0C.min^{-1}$.

2.3. Porosity & surface analysis

Adsorption isotherms were accomplished from nitrogen adsorption at -196^{0}C over the processed activated carbon utilizing an automatic adsorption apparatus (Nova 3000e series, USA). Brunauer–Emmett–Teller (BET) equation was applied for determining the relative pressure (P/P^0) within 0.05 – 0.2. The obtained results from the isotherms were applied to define the S_{BET}. The Horvath–Kawazoe (HK) method was applied to determine the micropore volume. The pore size division and the mesopore volume were defined using the Barrett–Joyner–Halenda (BJH) design.

2.4. Ultimate and Proximate analysis

The cinnamon, char, and prepared CSAC samples' proximate analysis were conducted using (TGA; Perkin Elmer TGA 7). The proximate analysis was studied according to. For CHN-O elemental analysis, about 30–50 mg of a sample was analyzed, and the data was recorded using a Perkin-Elmer Series II CHNS/O Analyser model 2400.

2.5. FTIR analysis

The samples' FTIR spectra were registered between 4000 and 450 cm^{-1} in a mobile IR- portable FT-IR (Bruker Optics). This measurement was used for the starting material (cinnamon stick), char, and CSAC samples. Firstly, before the analysis, samples were dried out in an oven at 50–60°C (at atmospheric pressure) for 3–5 hours for complete water removal.

2.6. SEM analysis

Surface morphology was surveyed utilizing a scanning electron microscope (SEM) ZEISS, EVO-MA10.

2.7. Adsorption equilibrium studies

In a set of 100 ml conical Erlenmeyer flasks, by adding a 25 ml solution of different initial concentrations (20-50 mg/L) CPS in acetonitrile adsorption isotherms were performed. An orbital shaker (SI-300R) continually stirred the mixture [3]. Similar masses of activated carbon (0.1 g) of mesh size (18*30) were attached. Samples were regularly-obtained every 10 min, and the concentration of CPS was defined by applying a double beam UV-Vis Spectrophotometer (Shimadzu, Japan). A wavelength of about 289 nm (λ_{max}) was adopted for all absorbance examinations for all specimens. For measurement of the removal capability (%) R, Eq*(1)* was adopted:

$$\%R = \frac{C_0 - C_t}{C_t} \times 100 \quad (1)$$

Where C_o and C_t (ppm) imply the initial concentration and concentration at time interval *t*.

The highest adsorption potential at equilibrium, q_e (mg. g^{-1}), was calculated applying Eq. (2):

$$q_e = \frac{(C_0 - C_e)v}{w} \quad (2)$$

Where C_e (mg. L^{-1}) signifies the concentration after the equilibrium of the CPS solution, w denotes the adsorbent mass (g), and v signifies CPS solution volume (L).

3. Results and discussion

3.1. Ultimate and Proximate analysis

The ultimate and proximate examinations of the raw-material, char, and CSAC specimens are seen in Table 1. The results revealed that the raw-material gives extended carbon content, high volatile material, and low-ash content, which is an excellent candidate for producing activated carbon. The liberation of rising volatile material by carbonization and activation were the targets, ending in chars and initiated carbon, a carbon element. The humidity percent in the chars and CSAC did not show any unusual model with different pyrolysis and activation because all these processes were done over 100°C. Consequently, their dehydration impacts would most reasonably be related to the various specimens.

Table 1. Properties of raw material, char, and CSAC samples.

Sample	Ultimate (wt.% dry-ash-free basis)				Proximate (wt.%)			
	C	H	N	O	Moisture (%)	Volatiles (%)	Carbon (%)	Ash (%)
Raw material (cinnamon)	46.35	18.65	0.32	34.68	7	70	21.6	1.40
Char	68.09	1.08	0.45	30.38	7.5	28	62.48	1.49
(CSAC)	80.05	0.92	0.58	18.45	8	11	79.48	1.52

3.2. FTIR analysis.

Surface groups created by heteroatoms attached to the carbon atoms provide additional chemical characteristics. Infrared spectroscopy presents knowledge on the chemical composition and the same functional groups of the carbon element. Figure 1 shows FTIR spectra for different samples showing the difference between the raw cinnamon, char, and the CSAC. The prominent specimen peak located at 3570– 3000 cm^{-1} represents the (–OH) group and may be accompanying to the water adsorbed. The different peaks cannot solely be relevant to certain specific groups. It is appropriate that the 1460 –1490 cm^{-1} peak agrees to the (–CH–) group, the 1603 cm^{-1} peak describes the aromatic group, and the (C- O-C) group should be located between 1000 and 1300 cm^{-1} (many peaks look in this interval). For the char and CSAC samples, the challenging preparation conditions of temperature treatment in inert and oxidizing environments, respectively, end in a large variety of the peak strengths of all the related definite absorption bands, commonly with peak ever-changing or peak merging. This is because of converting the organic form of cinnamon into a nearly-absolute carbon construction by eliminating any lasting of oxide and hydrogen groups at these higher temperatures.

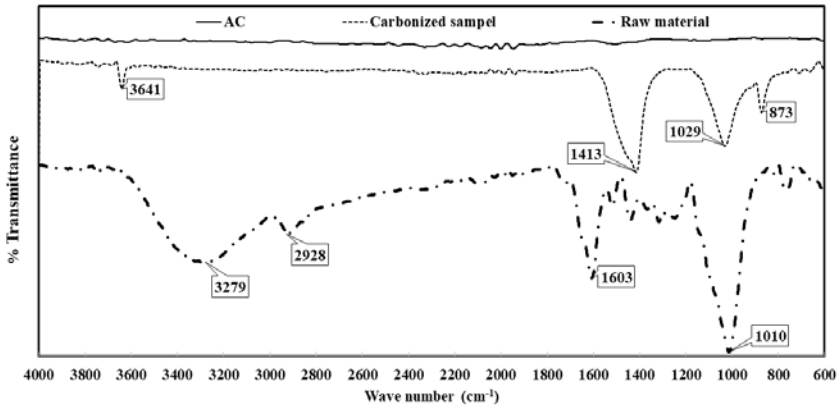

Figure 1. FTIR Spectra for the raw material, char, and CSAC samples

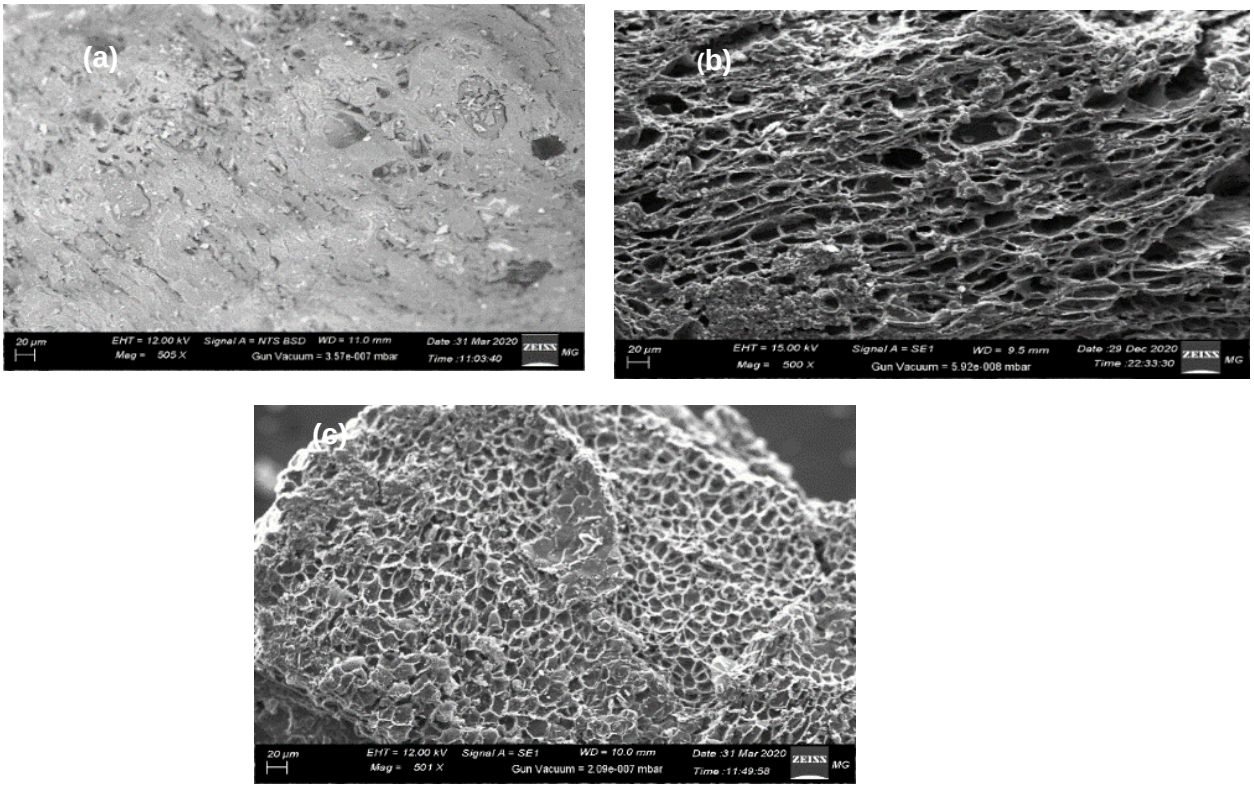

Figure 2. SEM images of (a) raw material (b) carbonized sample (c) CSAC.

3.3. SEM study for the preparation of CSAC.

Figure 2 a, b, and c illustrate the sample's SEM picture before and after the process of pyrolysis and activation. Porous solid is formed through these two processes. In general, during pyrolysis and cinnamon activation, the largest of the non-carbon components, hydrogen, and oxygen are primarily-extracted in volatile mode by the pyrolytic breakdown of the initial components. The innocent atoms of primary carbon are classified into fixed crystallographic structures recognized as elementary graphite crystallites. The crystallite's shape is different so that free spaces (pores) endure among them.

3.4. Yield, pore size, and surface area study

3.4.1. Impact of pyrolysis. The CSAC's surface area and micropore volume were the primary indicators for determining pyrolysis's most appropriate conditions. The yield was further brought into concern when choosing these excellent states. In this research, a dual-stage tuning was applied. The initial step or the primary optimization method was to choose a suitable condition for the pyrolysis temperature. When the pyrolysis temperature parameter had been optimized, its benefit would be applied for following activation tests in which one of the other parameters to be optimized was different (hold up time) whilst maintaining the balance fixed. The Impact of the temperature of pyrolysis on the surface area, carbon yield, and porosity of the char samples are given away in Figure 3 and Table 2.

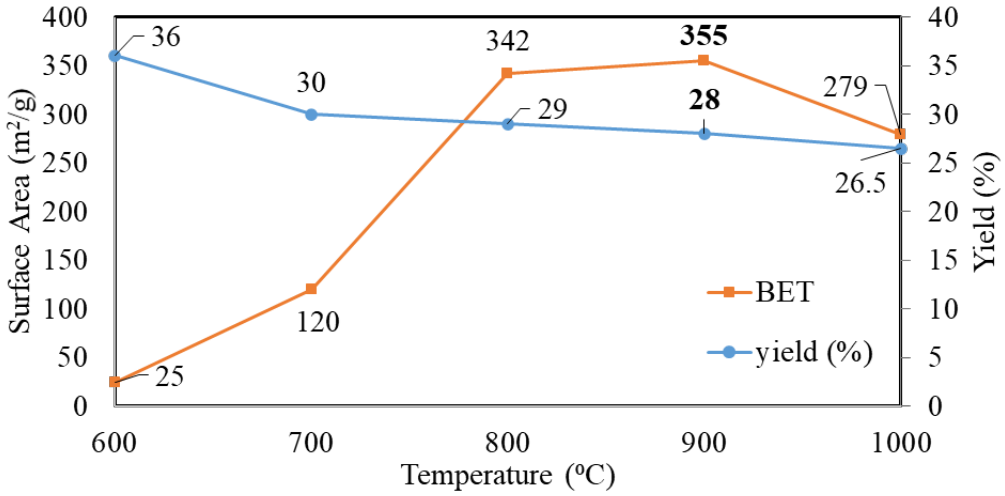

Figure 3. Effect of pyrolysis temperature on the BET surface area ($m^2.g^{-1}$) and the yield of carbonised samples

Table 2. Surface area ($cm^3.g^{-1}$) and porosity ($m^2.g^{-1}$) volume distribution of carbonized samples.

Sample	S_{BET} (m^2/g)	Pore volume (cm^3/g)				Mean pore diameter (nm)
		Total pore volume	Micropore volume	Meso pore volume	Macro pore volume	
600 ^{0}C	25	0.029	0.008	0.021	0	4.83
700 ^{0}C	120	0.087	0.037	0.045	0.005	3.45
800 ^{0}C	342	0.196	0.137	0.047	0.012	2.58
900 ^{0}C	355	0.198	0.144	0.046	0.008	2.23
1000 ^{0}C	279	0.173	0.129	0.043	0.001	2.48

Figure 4 demonstrates the isotherms of the different carbons prepared under unlike pyrolysis temperatures. Nitrogen adsorption at 77 K increased with increases in pyrolysis temperature from 600 to 900 ^{0}C. This is because the pore volume and surface area (BET) have increased from 0.029 to 0.198 cm^3/g and 25 to 355 m^2/g. However, any increase in the pyrolysis temperature (1000 ^{0}C) leads to a reduction in the nitrogen (N_2) adsorption due to decreased surface area (S_{BET}) and total pore volume to 279 m^2/g 0.173 cm^3/g, respectively.

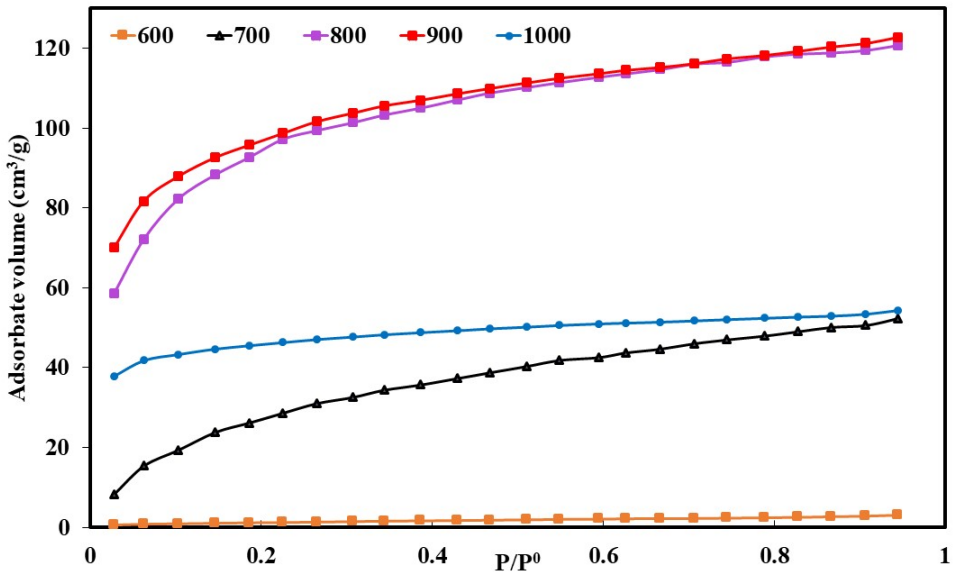

Figure 4. Isotherms of char samples prepared under different pyrolysis conditions [600-700-800-900-1000 denotes pyrolysis temperature (°C)].

3.4.2. Process of Physical Activation. At this step of the work, the pyrolyzed sample at 900°C, which has a profusely surface area, was chosen for seeking the Impact of the activation progression. Time of activation affects the surface area, and porosity, as presented in Table 3. the BET surface area's optimum values and total porosity were at holding time for 2h.

Table 3. The surface area by BET method and pore volume distribution for CSAC samples.

Sample	S_{BET} (m^2/g)	Pore volume (cm^3/g)				Mean pore diameter (nm)
		Total pore volume	Micropore volume	Meso pore volume	Macro pore volume	
30 min	640	0.32	0.254	0.062	0.004	2.31
45 min	652	0.36	0.257	0.1	0.003	2.55
60 min	696	0.37	0.278	0.054	0.038	2.46
90 min	842	0.455	0.33	0.125	-	2.51
120 min	**894**	0.49	0.35	0.14	-	2.67
150 min	741	0.38	0.29	0.087	0.003	2.48

Figure 5 demonstrates the isotherms at 77 K by N_2 adsorption for CSAC created by physical activation using CO_2. All isotherms of all activated carbons series belong to a union of type (I) and (IV) isotherm, rendering to IUPAC. Moreover, the nitrogen uptake significantly-improves at a much more crucial relative pressure. The adsorption of nitrogen increased with increases of activation hold-up time from 30 to 120 min due to increased porosity and surface area. However, protracted activation of the sample at a temperature of 900°C and a staying at this temperature for 150 min leads to diminishing porosity and surface area and, consequently, the nitrogen adsorption (Table 3).

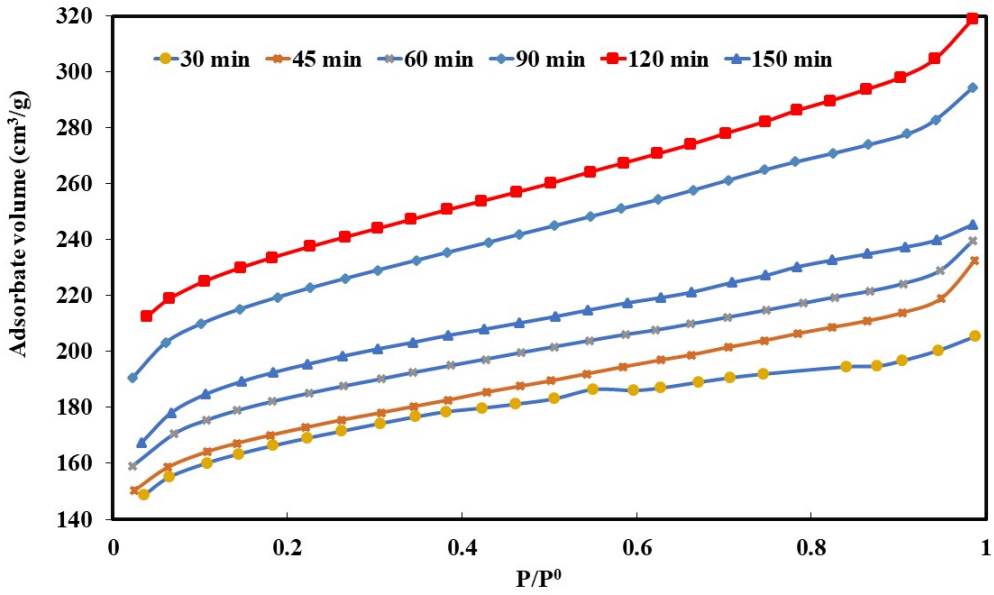

Figure 5. Adsorption isotherms of CSAC samples at 900^0 C under a different holding time [30-45-60-90-120-150 min].

3.5. Batch adsorption studies

Chlorpyrifos (CPS) is used in most agrochemicals in urban areas as an organophosphorus compound. CPS is extant in various forms, such as condensed emulsions, wet-table powders, granules, dust, controlled-release polymers, etc.[3].

3.5.1. Impact of CPS's initial concentration. In this part of the work, the optimized prepared sample was chosen for studying CPS adsorption. This sample displays the uppermost surface area, 894 m^2/g, and a whole pore volume of 0.49 cm^3/g. The adsorption of CPS by CSAC was studied at different initial CPS concentrations (20,30,40, and 50ppm). The experimentations were conducted out at a fixed adsorbent(CSAC) dose (0.1 g), at room temperature (25 ±1 ºC), pH (7.0), and 100 rpm. Figure 6 demonstrates the result for the outcome of CPS's initial concentration adsorption onto CSAC. According to the sorting of adsorption isotherms, the adsorption of CPS by the CSAC is of class L (Langmuir-type)[4]. The maximum value of sorption capacity was detected at 50 ppm. The adsorption capacity improved increasingly as the concentration increased because of the vital role of initial concentrations on the adsorption of CPS on AC[5]. Figure 7 demonstrates the result of the CPS initial concentration effect on the elimination efficiency by CSAC samples. The initial CPS concentration-effect hinge on the direct relationship between the CPS concentration and the existing accessible sites on the exterior of an adsorbent [6]. Frequently, the rate of CPS replacement declines with an improvement in initial dye concentration, which maybe because of the fullness of adsorption places on the adsorbent exterior [7]. At low concentration, there will be unfilled active places on the adsorbent cover, and when the first CPS concentration develops, the active places needed for adsorption of the CPS molecules will close [8]. Still, the development in the original CPS concentration will improve the adsorbent's filling quantity on the surface of the CSAC, which may be due to the great driving power for mass at a tremendous primary CPS concentration [9].

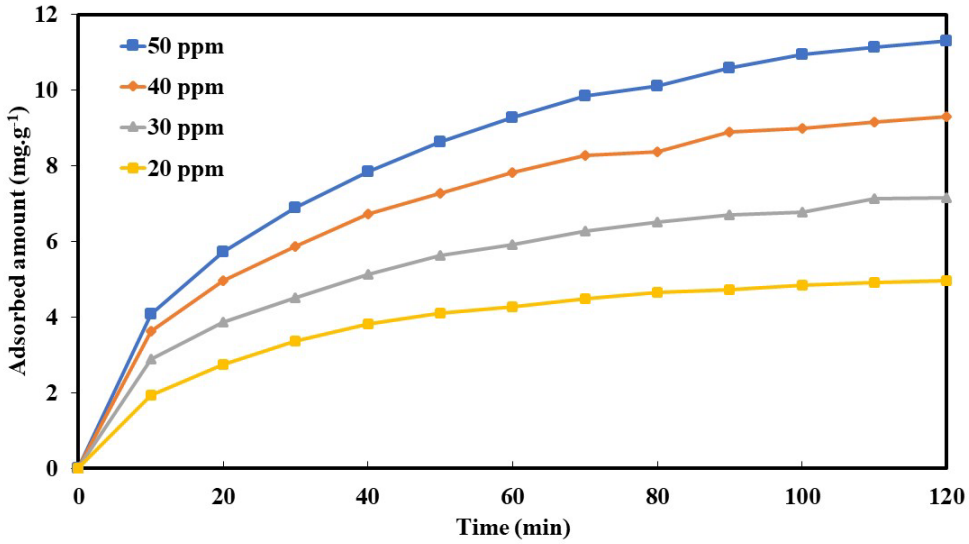

Figure 6. Initial adsorbate concentration effect on the extreme adsorption capacity of CPS using CSAC.

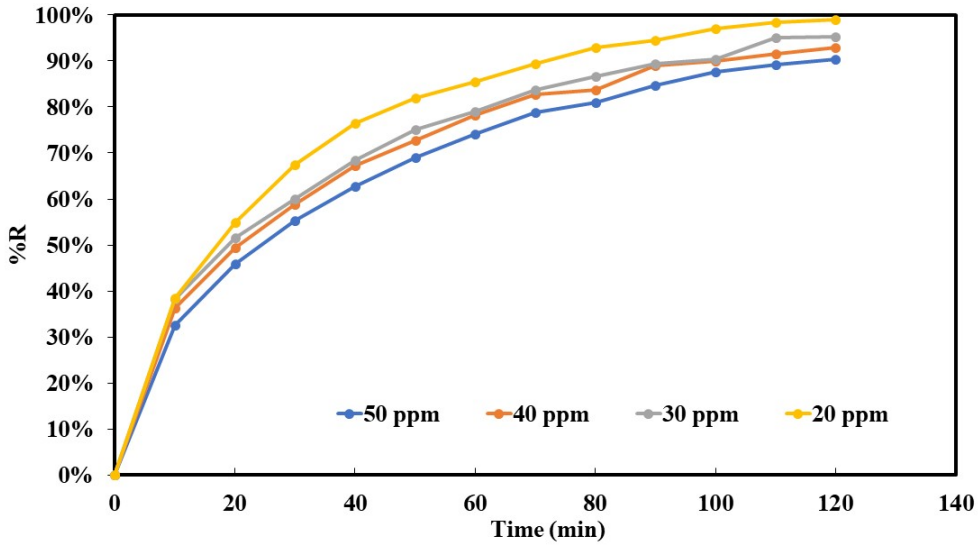

Figure 7. Effect of initial adsorbate concentration on the % removal of CPS using cinnamon sticks-based AC.

3.5.3. Adsorption Temperature consequence on the elimination of CPS. As demonstrated in figure 8, the adsorption of CPS onto CSAC samples decreases with temperature increase, indicating an exothermic process. This decrease of removal at high temperature possibly is due to the adsorption forces' failing between the surface of CSAC and the CPS species' active sites and between adjacent CPS molecules on the adsorbed phase[10].

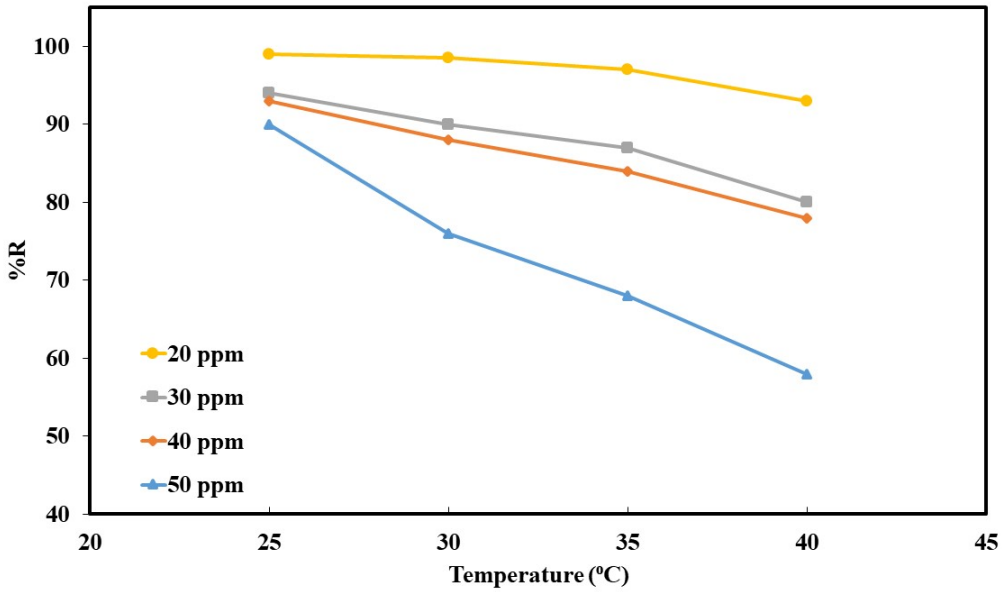

Figure 8. Effect of temperature on the removal of CPS with different initial concentrations.

3.6. Adsorption equilibrium isotherms

Three isotherms were verified for their capability to define the investigational consequences, namely the Langmuir, Freundlich, and the Temkin isotherm. Eq (3) expresses the Langmuir model.

$$\frac{C_e}{q_e} = \frac{1}{q_{max} \cdot K_L} + \frac{C_e}{q_{max}} \quad (3)$$

Where q_e(mg/g) and C_e(mg.L^{-1}) are the CPS adsorbed amount per unit mass of CSAC and CPS concentration at steadiness, respectively. q_{max} is the maximum quantity of the CPS per gram CSAC to form an entirely monolayer perfusion on the surface-bound at high C_e, and the constant K_L is referred to as the binding sites' affinity (L.mg^{-1}). The outline of specific adsorption (C_e/q_e) against the steadiness concentration (C_e) (figure 9) illustrates that the adsorption conforms to the Langmuir model. The Langmuir constants q_{max} and K_L were determined from the plot's slope and intercept and are existing in Table 4. The separation factor R_L is considered one of the critical characteristics of the Langmuir isotherm that is donated by Eq (4).

$$R_L = \frac{1}{1 + K_L C_0} \quad (4)$$

Where; C_0 is the uppermost initial CPS concentration (mg/L), and K_L (L/mg) is Langmuir constant. The R_L value is a sign of the form of the isotherm to be whichever unfavorable ($R_L > 1$), linear ($R_L = 1$), irreversible where ($R_L = 0$), or favorable ($0 < R_L < 1$). The values of R_L between 0 and 1 specify favourable adsorption. R_L's value in the current search was found to be 0.0154, demonstrating that the adsorption of CPS on CSAC is favourable.

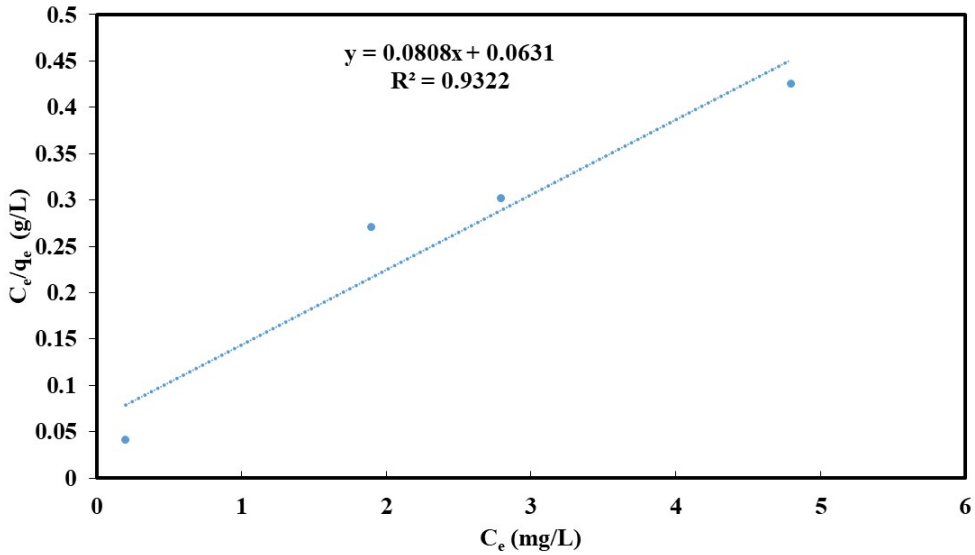

Figure 9. Langmuir adsorption isotherm of CPS on CSAC.

Eq (5) is used to describe a heterogeneous system (Freundlich isotherm) [5].

$$log\ q_e = log\ K_F + \left(\frac{1}{n}\right) log\ C_e \quad (5)$$

Where K_F and n are, Freundlich coefficients with K_F (mg/g (L/mg)$^{1/n}$) are the sorbent's adsorption capacity, and n indicating how is adsorption is esteemed. The extent of the exponent 1/n gives favourable adsorption. Values of n more than 1 represent favourable adsorption. Values of n and K_F are computed from the plot's slope and intercept (figure 10) and recorded in Table 4.

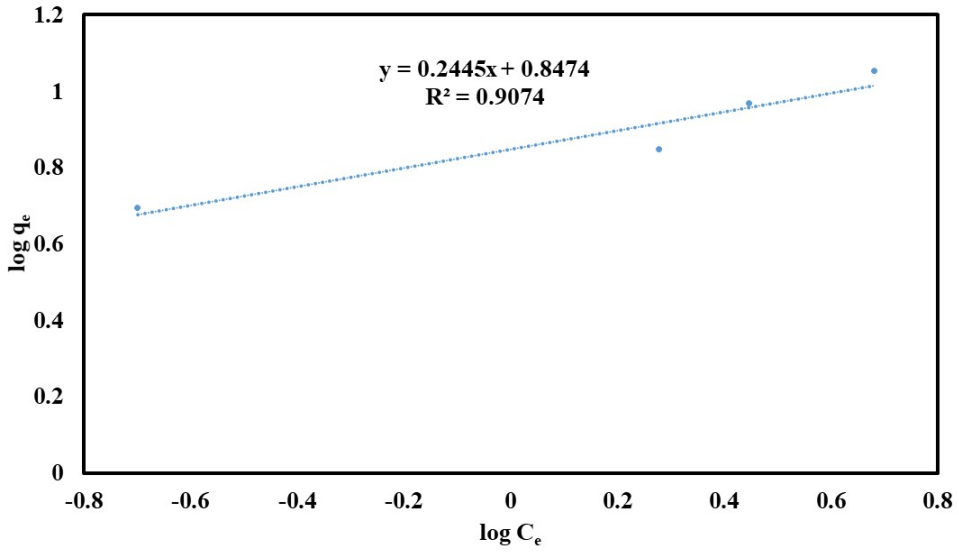

Figure 10. Freundlich adsorption isotherm of CPS on CSAC.

The Temkin isotherm is expanded for the determination of physical or chemical sorption characteristics. It has generally been applied in the linear form as described in Eq (6).

$$q_e = \frac{RT}{b} \ln K_T + \frac{RT}{b} \ln c_e \quad (6)$$

Where b is a constant link to the sorption heat (J/mol), K_T is the Temkin isotherm constant (L/g), R the gas constant (8.314 $J.mol^{-1}K^{-1}$), and T the absolute temperature (K). Therefore, by plotting q_e versus ln C_e (figure 11), the constants K_T and b can be determined. The constants K_T and b are listed in Table 4. If the heat of the sorption value is less than 1.0 kcal/mol, then physical adsorption occurs. Besides, its value of 20-50 kcal/mol, then chemical adsorption is occurring. If the sorption value is in-between (1 - 20 kcal/mol), then both chemical and physical adsorption is entangled in the adsorption. As it can be seen in Table 4, the Langmuir model's isotherm matches fairly well with the investigational data (correlation coefficient $R^2 > 0.93$). The capacity of monolayer CPS sorption rendering to this model was 12.37 $mg.g^{-1}$. This is owed to the homogeneous distribution of active sites onto the CSAC surface since the Langmuir equation suppose that the surface is similar or homogenous.

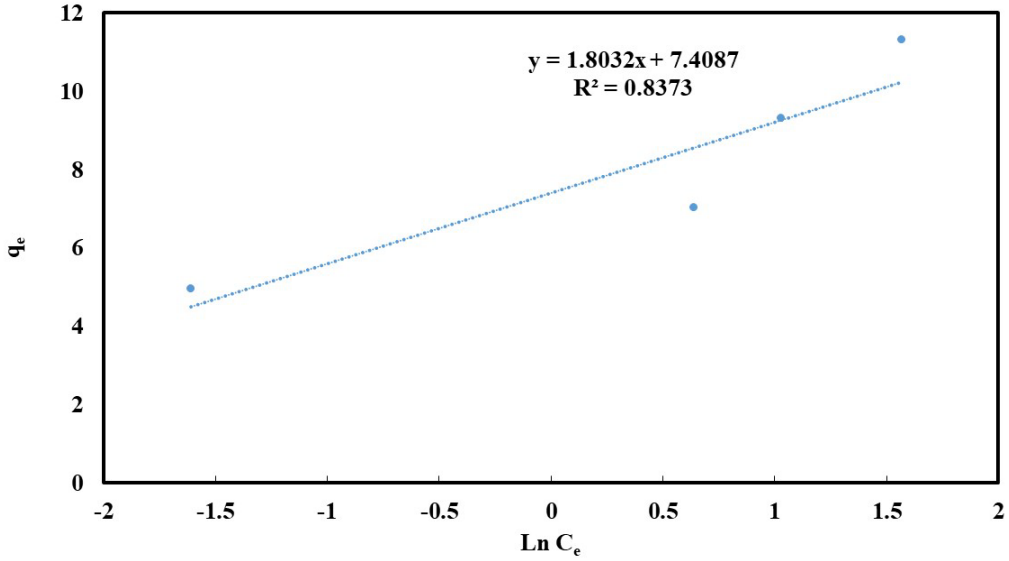

Figure 11. Temkin adsorption isotherm of CPS on CSAC

Table 4. Isotherm parameters for removal of CPS by CSAC

Isotherm	Parameters
Langmuir	
q_{max}(mg/g)	12.37
K_L(L/mg)	1.28
R_L	0.0154
R^2	0.9322
Freundlich	
K_F	7.04
n	4.09
R^2	0.9074
Temkin	
K_T	1.413
b(kJ/mol)	1.373
R^2	0.8373

3.7. Adsorption kinetics

Kinetic adsorption results for different CPS concentrations were examined using a pseudo-first-order (PFO) model and a pseudo-second-order (PSO) model. For the PFO kinetic model, k_1 values were obtained from the linear log plots' slopes (q_e-q_t) against t (figure 12). The values obtained for the correlation coefficient were comparatively small. The values of experimental q_e were not compatible with the estimated values obtained from the linear plots, as perceived in Table 5. This demonstrates that the sorption of CPS to CSAC did not conform to the PFO equation.

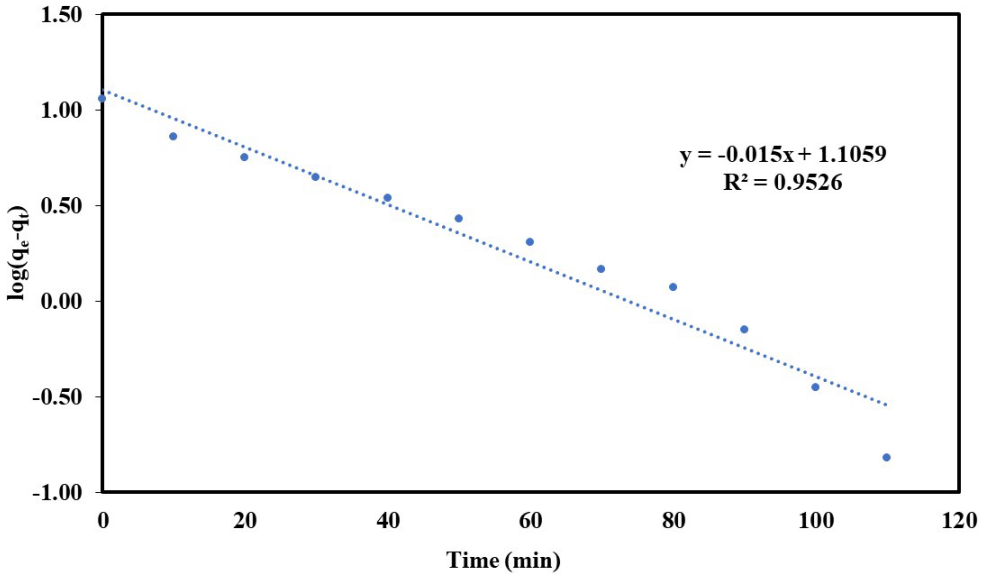

Figure 12. Pseudo-first-order kinetics for CPS adsorption onto CSAC at 25 ˚C.

But for the (PSO) pseudo-second-order kinetics, the linear plot of t/q_t against t, as seen in figure 13, indicates a strong relationship between the investigational and the measured q_e values (Table 5). Besides, the correlation coefficients for the PSO model were larger than 0.99 for the adsorption of CPS, indicating the applicability of this model to explain the CPS sorption mechanism on the CSAC samples.

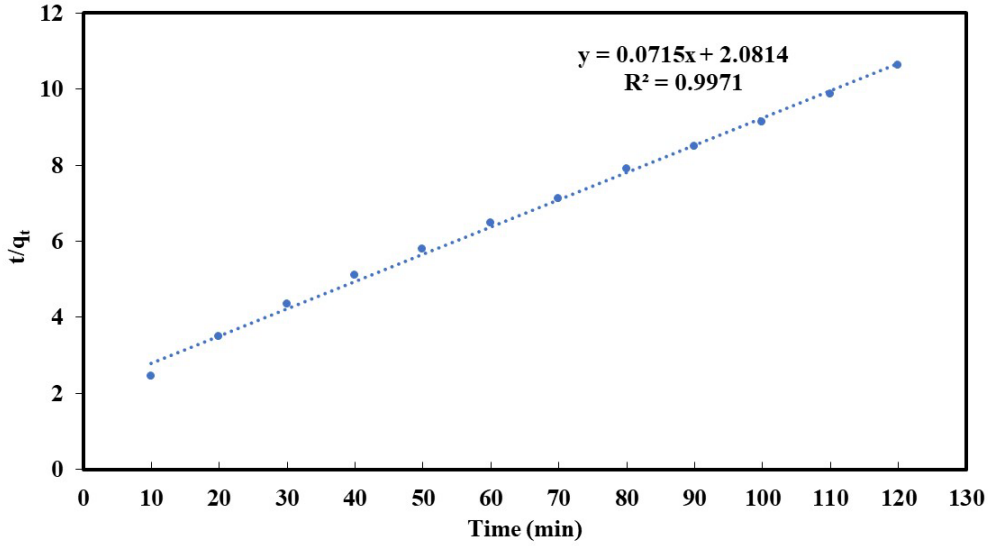

Figure 13. Pseudo-second-order (PSO) kinetics for adsorption of CPS onto CSAC at 25 ˚C.

Table 5. Adsorption kinetic parameters

Kinetic model	parameters	value
Experimental	q_t	11.3
Pseudo first order (PFO)	q_e	12.76
	k_1	0.0345
	R^2	0.9526
Pseudo-second-order (PSO)	q_e	13.98
	k_2	0.0025
	R^2	0.9971

3.8. Design of water recycling system based on the batch sorption process

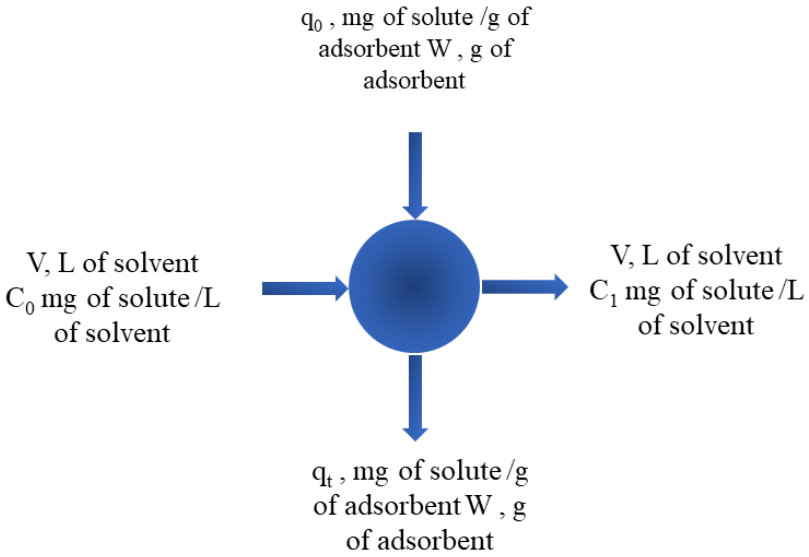

Figure 14. A single-stage water recycling batch adsorber

Figure 14 depicts a representation diagram of a single-step process (batch sorption). The effluent holds V (L) of wastewater and a CPS initial concentration C_0 is reduced to C_1 in the adsorption process. In the management stage W (g) CSAC is added to the solution, and the adsorbate concentration on the CSAC deviations from $q_0 = 0$ (at the beginning) to q_1. Eq. 7 shows the mass balance for the adsorbate in a single-stage water recycling system.

$$V(C_0-C_1) = W(q_0- q_1) \quad (7)$$

Under equilibrium conditions, $C_1 \rightarrow C_e$ and $q_1 \rightarrow q_e$

$$VC_0+Wq_0 = VC_e + Wq_e \quad (8)$$

For the adsorption of CPS on CSAC. The Langmuir isotherm best reflects experimental results. As a result, the equation works better when q_1 is replaced in the repositioned form of Eq.*(8)*, giving adsorbent material/solution shares for this certain system,

$$\frac{W}{V} = \frac{(C_0 - C_1)}{q_e} = \frac{C_0 - C_e}{q_{max} K_L C_e / (1 + K_L C_e)} \quad (9)$$

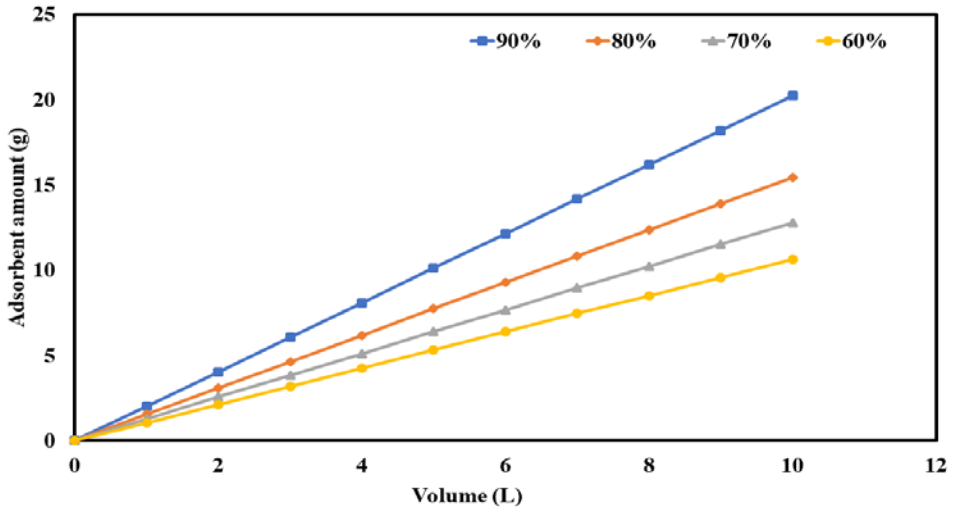

Figure 15. Adsorbent mass (W) against the volume of effluent (V) treated for different percentages of CPS removal

Figure 15 shows a sequence of plots (60, 70, 80, and 90% CPS removal at different solution volumes, i.e., 1, 2, 3, 4, 5, 6, 7, 8, 9, and 10 L) derived from Eq. (9) for the adsorption of CPS on CSAC at the primary concentration of 20 ppm. The amount of CSAC required for the 90% removal of CPS solution of concentration 20 mg/L was 2.01, 4.02, 6.07, and 8.09 g for CPS solution volumes of 1, 2, 3, and 4 L, respectively.

4. Conclusions

This study revealed that water recycling systems used in space flights could depend on the usage of the prepared CSAC. Besides, CSAC is cost-effective and considered an encouraging adsorbent for wastes such as CPS discharge across a broad array of concentrations. The surface area was moderately-high (894 m^2/g) with a high pore volume (0.49 cm^3/g) and was observed to be micro-porous (V_{mic}= 0.35 cm^3/g). Equilibrium data were related to Langmuir, Freundlich, and Temkin isotherms. The data were adequately-represented by the Langmuir isotherm form, with the highest monolayer adsorption potential of 12.37 mg/g at 25°C. The maximum monolayer adsorption capacity reduced with rising temperature proved the exothermic character of the adsorption cooperation. The adsorption kinetics was decided to closely-reflect the pseudo-second-order kinetic design. The adsorption completion of the CSAC was similar to the popular charcoal and some other adsorbents described in related investigations.

References

[1] J. W. Fisher, S. Pisharody, M. J. Moran, K. Wignarajah, Y. Shi, and S.-G. Chang, 2000, "Reactive carbon from life support wastes for incinerator flue gas cleanup," *SAE Technical Paper*0148-7191,.

[2] A. SE, C. Gimba, A. Uzairu, and Y. Dallatu, 2013"Preparation and characterisation of activated carbon from palm kernel shell by chemical activation," *Research Journal of Chemical Sciences* ISSN, vol. **2231**, p. 606X.

[3] M. M. Jacob, M. Ponnuchamy, A. Kapoor, and P. J. J. o. E. C. E. Sivaraman, 2020"Bagasse based biochar for the adsorptive removal of chlorpyrifos from contaminated water" *Journal of Environmental Chemical Engineering*, p. 103904.

[4] R. C. Bansal and M. Goyal, 2005, Activated carbon adsorption. CRC press.

[5] I. Tan, A. Ahmad, and B. Hameed, 2009,"Adsorption isotherms, kinetics, thermodynamics and desorption studies of 2, 4, 6-trichlorophenol on oil palm empty fruit bunch-based activated carbon," *Journal of hazardous materials*, vol. **164**, no. 2-3, pp. 473-482.

[6] L. Wang, Zhanga, J., Wang, A, 2008"Removal of methylene blue from aqueous solution using chitosan-g-poly (acrylic acid)/montmorillonite superadsorbent nanocomposite. *Colloids Surf.," A: Physicochem. Eng Aspects* **322**, 47-53.

[7] L. J. Yu, Shukla, S.S., Dorris, K.L., Shukla, A. and Margrave, J.L., 2003, "Adsorption of Chromium from Aqueous Solutions by Maple Sawdust," *J. Hazard. Mater.*, B**100**, 3-63.

[8] A. J. K. Algidsawi, 2011" A Study of Ability of Adsorption of Some Dyes on Activated Carbon From Date' S Stones," *Australian Journal of Basic and Applied Sciences*, **5**(11): 1397-1403.

[9] J. R. S. Annadurai G, Lee D. J. , Ruey-Shin Juang , Duu-Jong Lee., 2002, "Use of cellulose-based wastes for adsorption of dyes from aqueous solutions," *Journal of Hazardous Materials* B**92** , 263–274.

[10] S. Vigneshwaran, J. Preethi, and S. J. I. j. o. b. m. Meenakshi, 2019, "Removal of chlorpyrifos, an insecticide using metal free heterogeneous graphitic carbon nitride (g-C3N4) incorporated chitosan as catalyst: Photocatalytic and adsorption studies," *International Journal of Biological Macromolecules* vol. **132**, pp. 289-299.